A Comparison of Waveform Data from Different Altimeters

G.D. Quartly, M.A. Srokosz & A.C. McMillan

Southampton Oceanography Centre
Empress Dock, Southampton, SO17 3 SH, UK
gdq@soc.soton.ac.uk

Motivation

The mathematical formulation of an ideal waveform is very simple. The power in the waveform bins, P(t) is given by the convolution of three terms (*Brown*, 1977; *Hayne*, 1980):

$$P(t) = q(t) * P_{PTR}(t) * P_{FS}(t)$$

where the Point Target response, $P_{PTR}(t)$ is a replica of the emitted pulse, $P_{FS}(t)$ is the Flat Surface response and q(t) represents the distribution of surface scatterers, which for deep oceans can be assumed invariant within the altimeter footprint.

Although the $P_{PTR}(t)$ is normally a sinc function, it is usually adequate to represent it by a Gaussian. The Flat Surface response may be modelled as a decaying exponential for $t > 0$ (and equal to zero otherwise). Thus the *expected shape* of a waveform over typical ocean conditions would be as below.

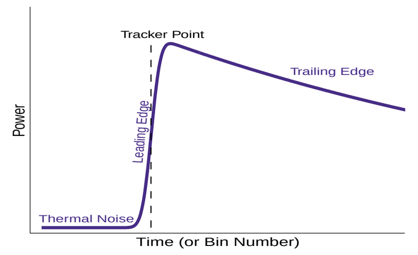

Given the *complete* time record for the received waveform and perfect knowledge of $P_{PTR}(t)$ and $P_{FS}(t)$ one would be able to determine the full description of the height of reflecting facets — not just the mean height and spread (i.e. sea level and wave height information) but also all the higher order terms such as skewness.

In practice one only has a finite number of waveform bins, and each of those has noise on it, whose amplitude is proportional to the true signal. Physically-based algorithms (e.g. the Maximum Likelihood estimator) have been developed which could derive higher-order terms of the sea surface height distribution, given such finite noisy data (*Tokmakian et al.*, 1994). However such algorithms depend upon the observed waveforms conforming to the theoretical model. Here we look at the characteristics of waveforms from some recent altimeters.

Non-oceanographic Applications

As well as the commonly-used techniques for deriving oceanographic parameters from altimeter data, there are a number of applications of waveform data in other areas of research. These include:

- Estimation of rain cell size, strength and structure (*Tournadre*, 1998; *Quartly*, 1998).
- Monitoring of the height of snow pack (*Bamber*, 1994, *Wingham* 1995a,b)
- Land elevation mapping (*Guzkowska et al.*, 1990)
- Monitoring water height of inland rivers and lakes (*Guzkowska et al*., 1990; *Birkett*, 1994)

For all of these the derivation of the required information is compromised if the characteristics of the waveform data do not conform to the theoretical model used.

Processing Technique

For the results displayed here we used a processing technique based on analysis of ensembles. If we had simply taken all data corresponding to a given wave height and processed to give mean waveform and its standard deviation, the analysis would be sensitive to secular changes. Principal amongst these are the equatorward/poleward differences for TOPEX (see later), instrumental mispointing (which will vary on time scales similar to the orbital period, and most affect the power returned in bins far from nadir, especially the last ones for TOPEX) and changes in overall signal strength due to variations in wind. This latter variation is especially important for Poseidon, since its AGC is only implemented in nominal increments of 1dB, so there is consequently ~20% variation in the power in particular wavebins on account of wind alone.

Here we take 10-second (~60 km along track) segments of waveform data, apply limited editing (to discard extreme events where the waveform is poorly positioned within the window due for example to rain events), and note the number of acceptable waveforms (passing editing criteria and having the same AGC scaling value). Provided there are sufficient, a mean waveform and its standard deviation are calculated for the ensemble, along with bin-to-bin correlations for the anomalies relative to the mean; they are then stored with the mean waveheight value for that segment.

Processing was done for approximately 1 day's data for each of the altimeters.

ERS-1

Launched 17th July 1991
Altitude ~780km
3dB beamwidth 1.3˚
PRF 1020 Hz
No. of pulses averaged per waveform: 50

ERS-2

Launched April 1995
Altitude ~780km
3dB beamwidth 1.3˚
PRF 1020 Hz
No. of pulses averaged per waveform: 50

Poseidon

Launched 10th August 1992
Altitude ~1336 km
3dB beamwidth 1.1˚
PRF 1650 Hz
No. of pulses averaged per waveform: 86 (53ms)

TOPEX (K_u)

Launched 10th August 1992
Altitude ~1336km
3dB beamwidth 1.1˚
PRF 4200 Hz
No. of pulses averaged per waveform: 456 (2x53ms)
Bins averaged in groups of 1, 2 & 4 prior to telemetry.
(Only equatorward data shown)

TOPEX (C)

Launched 10th August 1992
Altitude ~1336km
3dB beamwidth 2.8˚
PRF 1140 Hz
No. of pulses averaged per waveform: 240 (4x53ms)
Bins averaged in groups of 1, 2 & 4 prior to telemetry.
(Only equatorward data shown)

Mean Waveform

Ideally the mean waveform should have the shape illustrated above, with a flat non-zero thermal noise region, a rapidly rising leading edge (centred about the track point indicated by the dotted line) and a gradually tailing off plateau region. In reality it can be expected that there will be some droop at the end of the plateau and a rise at the beginning of the thermal noise on account of wrap-round in the on-board FFT.

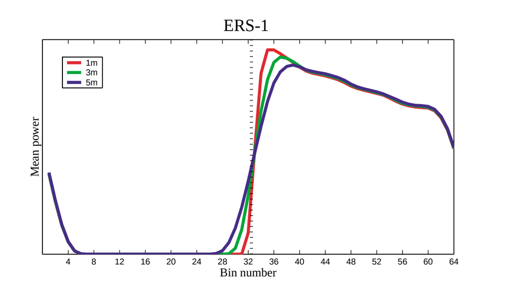

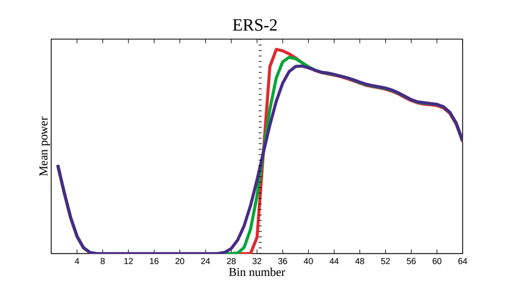

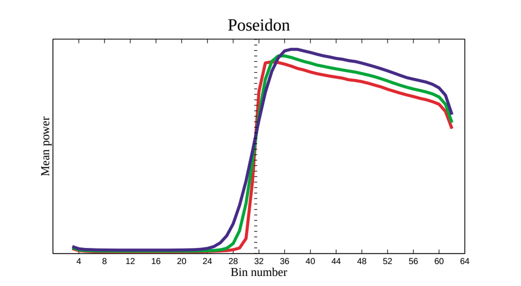

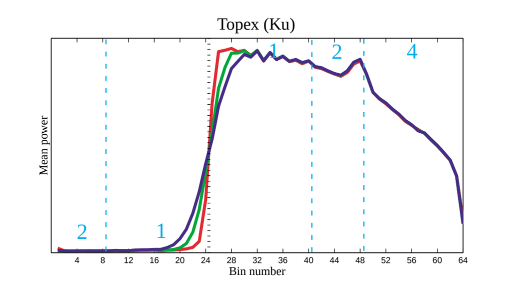

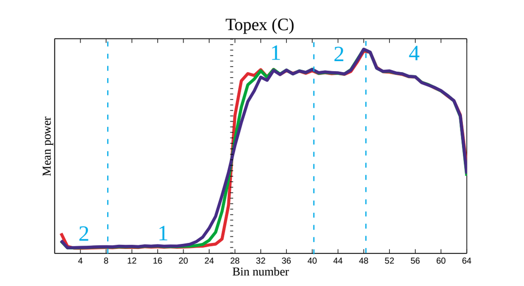

The mean waveforms for each altimeter show some departure from "ideal". The anomalies for TOPEX — both the spurious peak due to DC leakage and the saw-tooth on the plateau — are the most pronounced; however there is a definite 'waviness' (correlated bin-dependent amplification error) in the waveform shapes for ERS-1,2 and also Poseidon.

Std. Dev. of Waveform Ensemble

As the Rayleigh or 'fading' noise should be proportional to the mean signal, the standard deviation of the powers in each waveform ensemble should have the same shape as the mean.

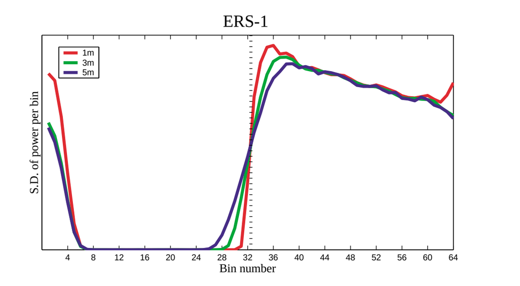

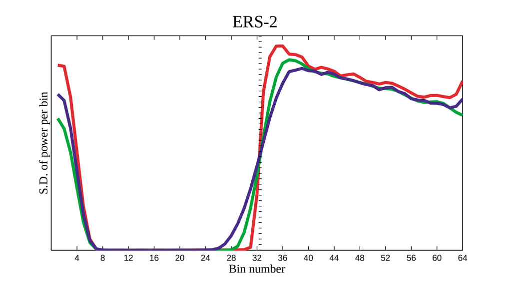

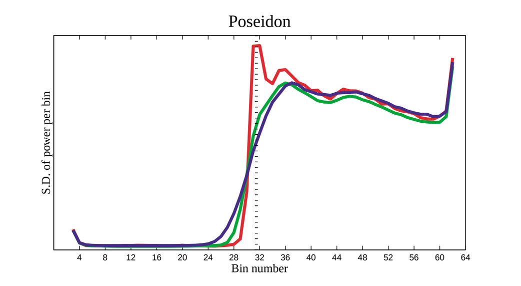

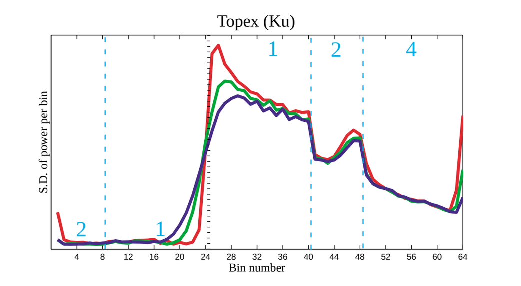

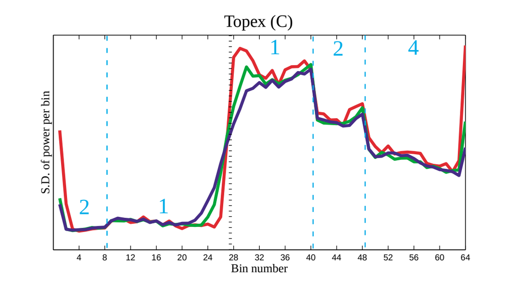

The standard deviation within waveform ensembles approximates to the shape of the mean waveforms (once allowance has been made for the step changes of $1/\sqrt{2}$ in the TOPEX data where the bin-averaging changes). The wrap-round leads to pronounced variability in the few first and last wavebins for ERS and TOPEX; these values have been excised from the supplied Poseidon data. Poseidon appears to show greatest variability just in front of the tracker point, possibly indicating that the waveform position is not so constrained by the on-board tracker as is the case for ERS and TOPEX.

Ratio of Mean to Std. Dev.

Each recorded waveform is the sum of N pulses. If each of these indvidual pulses has the same expected value at a given bin, and the variance of the Rayleigh noise is the same as the expected value, then the standard deviation of the mean of N_1 independent pulses should be the mean / $N_1^{0.5}$. Here we determine mean / S.D. and infer the effective no. of independent pulses, $N_1 = (\text{mean/S.D.})^2$. This will clearly always be less than the actual no. of pulses averaged together, N (which is indicated by the dashed line).

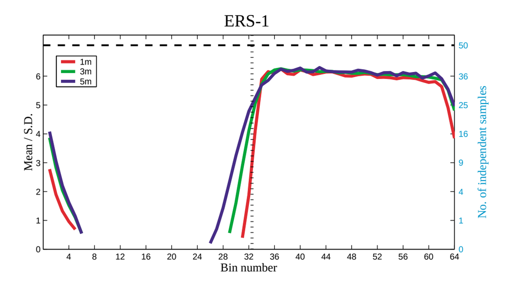

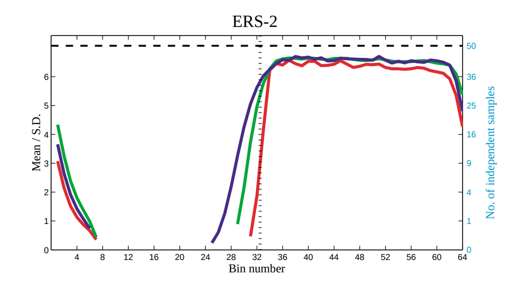

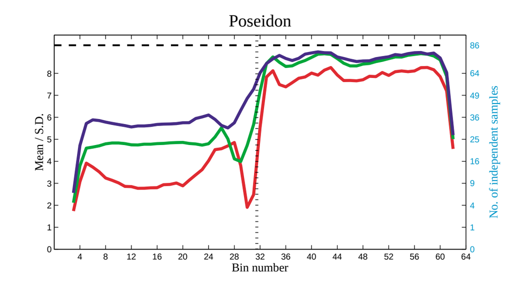

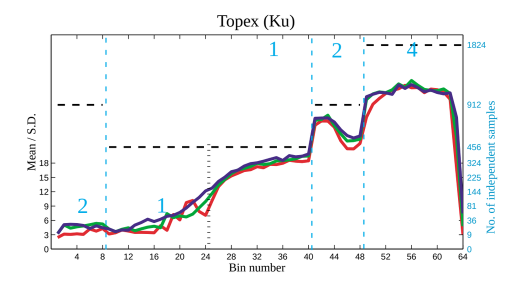

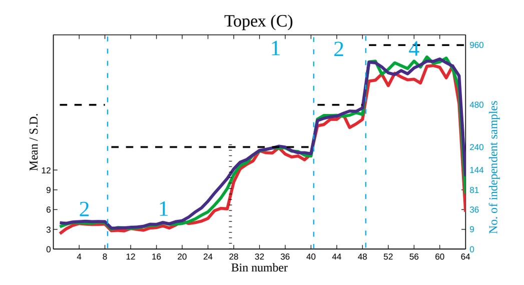

The plots for number of *independent* pulses per waveform show a constant plateaux for the trailing edges of ERS-1,2 and Poseidon waveforms, with the values being just below the number of pulses averaged. The values may be below the limit because the processing does not take account of secular changes within the ensembles. The improvement from ERS-1 to ERS-2 may be the result of the reduction in rounding errors. The small apparent no. of independent samples in Poseidon's thermal region is due to quantization in that region (the no. of counts per bin is typically 2±1). The strong dip prior to the track point is due to all returns coming from a small disc on the surface, for which the path lengths decorrelate less rapidly than for a large annulus. At low wave heights the effective reflecting region is smaller, so the no. of independent returns is less than at high wave heights.
The values for TOPEX are affected by the on-board averaging of consecutive bins in pairs or quartets. That the no. of independent pulses does change by a factor of 2 at these boundaries indicates that the powers in consecutive bins are independent. The K_u-band values are not close to the instrumental limit (shown by the dashed lines), because the pulse repeat interval is significantly less than the decorrelation time. These plots suggest that there will be no reduction in measurement noise if PRFs exceed ~3500Hz. For C-band, all pulses are independent.

Bin-to-bin correlations

Here we examine anomalies relative to the ensemble mean. As successive bins within a waveform represent reflections from different annuli on the surface, there should be no correlation in the Rayleigh fading for these different bins. However there may be instrumental effects or processing problems that give rise to such correlations. The illustrations shown here are for a wave height of 2m.

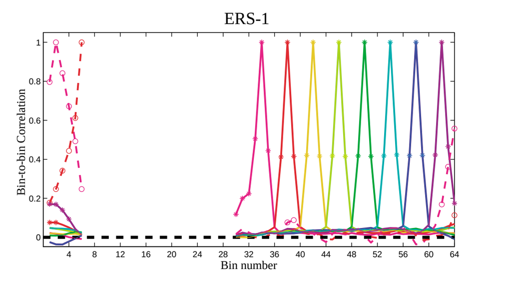

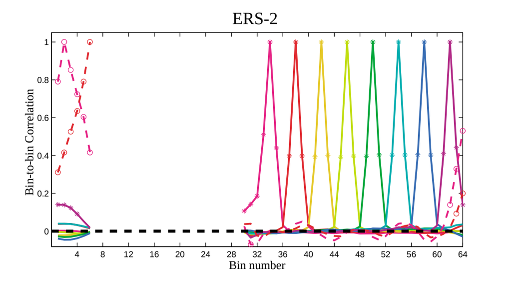

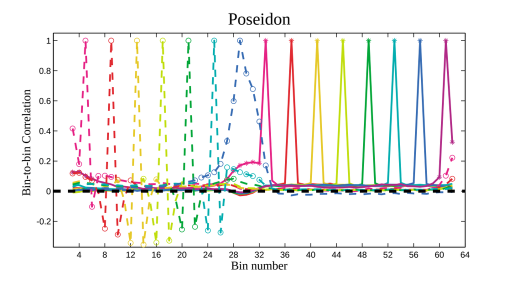

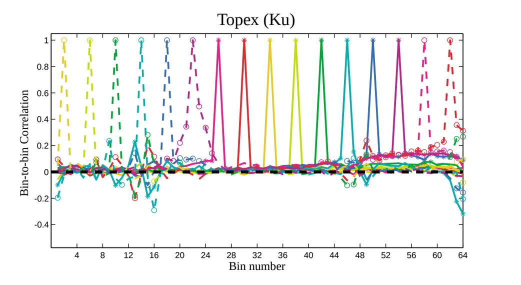

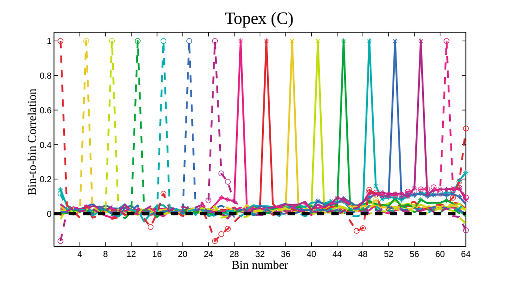

The waveforms showing the best decorrelation between consecutive bins are those for Poseidon. (There is however a strong anticorrelation between consecutive bins in the Poseidon thermal region, which cannot simply be explained away by the limited quantization). For the ERS altimeters, there is a pronounced (~0.4) correlation between the anomalies at consecutive bins, and some correlation between first and last bins on account of wrap-round. For the TOPEX data there are significant waveform-wide correlations in the last 16 telemetered bins for both K_u- and C-band. It is presently unclear whether these are instrumental effects (relating to the on-board averaging for example) or correspond to changes in environmental properties (e.g. wind roughening) at those bins furthest from nadir.

Summary for ERS-1

In the on-board processing on ERS-1 the strengths of individual returns were divided by 20 before summing in order to avoid overflow in the registers. Unfortunately in integer arithmetic this had the effect of reducing all the values prior to the leading edge to zero. Consequently it is impossible to determine the actual contribution of thermal noise elsewhere in the waveform.

Summary for ERS-2

The results are (not surprisingly) similar to those for ERS-1. The change in the on-board scaling of data (division by 10 rather than 20) prior to averaging appears to have resulted in an increase in the degree of independence of the summed waveforms.

Summary for Poseidon

The waveform data for Poseidon appear to be the most free of instrumental artefacts, possibly due to the use of solid state amplifiers rather than travelling wave tubes. The coarse quantization of the data means that there is some information lost at low noise levels, consequently the level of thermal noise cannot be estimated as accurately as for TOPEX.

Summary for TOPEX (K_u)

By using such a high PRF, TOPEX has increased our understanding of the decorrelation times between pulses. Unfortunately the instrument has been plagued by a number of other artefacts which make the processing and interpretation of its results more difficult:

i) The on-board averaging of bins in groups of 1, 2 or 4.

ii) The difference between equatorward and poleward sections

iii) The various power leakages, especially the strong DC leakage near bin 48 of the telemetered data.

Summary for TOPEX (C)

The TOPEX C-band information has been an almost neglected dataset, which is surprising given its quality. It suffers from the same 3 problems as the K_u-band of TOPEX, but does have the advantages:

a) It is less sensitive to mispointing on account of its broader beamwidth

b) Its waveforms are less susceptible to effects of rain (Quartly, 1997).

References

Bamber, J.L (1994) 'Ice sheet altimeter processing scheme' IJRS, **15**, 925-938.

Brown, G.S. (1977) 'The average impulse response of a rough surface and its applications' J. Oceanic Eng., **2**, 67-74.

Guzkowska M.A.J. et al., (1990) 'Developments in inland water and land altimetry' ESA Report.: XXX.

Hayne, G.S. (1980) 'Radar altimeter mean return waveforms from near-normal-incidence ocean surface scattering' Ant. Propagat., **28**, 687-692.

Quartly, G.D. (1997) 'Achieving accurate altimetry across storms: Improved wind and wave information from C-band' JAOT, **14**, 575-585.

Quartly, G.D. (1998) 'Determination of oceanic rain rate and rain cell structure from altimeter waveform data' JAOT, **15**, 1362-1379.

Tokmakian R.T. et al. (1994) 'The U.K. EODC ERS-1 altimeter oceans processing scheme' IJRS, **15**, 939-962.

Tournadre, J.(1998) 'Determination of rain cell characteristics from the analysis of TOPEX altimeter echo waveforms' JAOT, **15**, 387-406.

Wingham D.J. (1995a) 'A method for determining the average height of a large topographic ice sheet from observations of the echo received by a satellite altimeter' J. Glaciol., **41**, 125-141.

Wingham D.J. (1995b) 'The limiting resolution of ice-sheets derived from pulse-limited satellite altimetry' J. Glaciol., **41**, 413-422.

Acknowledgments

We thank ESA, CNES and NASA for the collection of these datasets. The ERS Waveform Product (WAP) data were provided by the UK PAF; Poseidon data by AVISO (with the assistance of Patrick Vincent) and the TOPEX Sensor Data Records (SDR) by Robert Benada of PO.DAAC. We were also helped greatly by discussions with George Hayne.